EVIDENCE AND PROSPECTS FOR THE RARE DECAY $K^+ \to \pi^+\nu\bar{\nu}$ AT BNL E787

George Redlinger*
TRIUMF, 4004 Wesbrook Mall
Vancouver, B.C., Canada V6T 2A3

Representing the E787 Collaboration

ABSTRACT

In 1997, E787 at Brookhaven National Laboratory (BNL) reported evidence for the rare decay $K^+ \to \pi^+\nu\bar{\nu}$ based on the observation of one event in the 1995 data set. The current status of this measurement is described.

*Supported by the Natural Sciences and Engineering Research Council of Canada.

1 Introduction

In the Standard Model (SM), quark mixing in weak decays and CP violation are related.[1] Detailed exploration of this relationship between two longstanding mysteries of particle physics is one of the major themes of experimental work in the field over the next decade(s). The rare decay $K^+ \to \pi^+\nu\bar{\nu}$ has drawn interest in this effort due to the theoretically clean relationship between the branching ratio and the poorly measured quark mixing parameter $|V_{td}|$. The intrinsic theoretical uncertainty in the branching ratio (arising mainly from QCD corrections to the charm contribution to the process) is estimated[2] to be about 7% for a given set of SM input parameters m_t, $|V_{cb}|$, and $|V_{td}|$. Stated differently, once the branching ratio for $K^+ \to \pi^+\nu\bar{\nu}$ is known, $|V_{td}|$ can be determined to $\sim 5\%$ (given perfect knowledge of m_t and $|V_{cb}|$). In the SM, the branching ratio is expected to be[3] $\mathrm{B}(K^+ \to \pi^+\nu\bar{\nu}) = (0.6 - 1.5) \times 10^{-10}$, using current data on m_t, m_c, V_{cb}, $|V_{ub}/V_{cb}|$, ϵ_K, and $\mathrm{B_d} - \overline{\mathrm{B_d}}$ mixing.

The E787 Collaboration at BNL presented evidence for $K^+ \to \pi^+\nu\bar{\nu}$ based on the observation of one clean event from data collected in the 1995 run of the Alternating Gradient Synchrotron (AGS).[4] The expected level of background in the signal region was 0.08 ± 0.03 events. However, the event also satisfied the most demanding criteria designed in advance for candidate evaluation; this put the event in a region where the expected background was 0.008 ± 0.005 events. If the event is due to $K^+ \to \pi^+\nu\bar{\nu}$, this would imply a branching ratio $B(K^+ \to \pi^+\nu\bar{\nu}) = 4.2^{+9.7}_{-3.5} \times 10^{-10}$, which is consistent with the SM range, although the central value is higher by a factor of about four.

Amongst the vast literature on non-SM physics with the signature $K^+ \to \pi^+$ "nothing," recent attention has focused on implications for electroweak symmetry breaking. R-parity conserving supersymmetry (SUSY) has been considered in many papers[5]; conclusions vary depending on assumptions, but a branching ratio two to three times above the SM level seems to be possible without going to exotic models. In R-parity violating SUSY,[6] $K^+ \to \pi^+\nu\bar{\nu}$ yields the best constraints on couplings relating the first two generations. Effects from top-color models[7] can also be significant.

The two-body decay $K^+ \to \pi^+X^0$, where X^0 is a long-lived noninteracting object, is indistinguishable experimentally from $K^+ \to \pi^+\nu\bar{\nu}$, except for the two-body kinematics. An interesting possibility is where X^0 is a Nambu-Goldstone boson from breaking some global symmetry, a well-known example of which is the familon[8] from the breaking of global family symmetry. The branching ratio is expected to be $B(K^+ \to \pi^+f) = 2.7 \times 10^{13}\ \mathrm{GeV}^2/F^2$, where F is the scale at which the symmetry is broken. Cosmological considerations lead to an upper bound[9] $F < 10^{12}$ GeV, implying $B(K^+ \to \pi^+f) \gtrsim 10^{-11}$. A new class of axion models has also recently been considered.[10]

In the late '60s, it was the absence of the process $K^+ \to \pi^+\nu\bar{\nu}$ (among others) at the then-expected rate which led to the "new" physics (GIM mechanism, charm, etc.) of the time and the eventual establishment of the SM. It would be poetic indeed if now a higher rate than expected were to be confirmed, leading the way beyond the SM.*
The remainder of this paper is organized as follows. We first remind the reader of the $K^+ \to \pi^+\nu\bar{\nu}$ detection strategy employed in E787, and of the results from the 1995 data. We then discuss the 1996 and 1997 runs, followed by a brief report on the status of the ongoing 1998 run and future plans.

2 Detection Strategy

2.1 The E787 Detector

The signature for $K^+ \to \pi^+\nu\bar{\nu}$ is a K^+ decay to a π^+ of momentum $P < 227$ MeV/c and no other observable product. Definitive observation of this signal requires suppression of all backgrounds to well below the sensitivity for the signal. Furthermore, reliable estimates of the residual background levels are needed.

Major sources of background include the two-body decays $K^+ \to \mu^+\nu_\mu$ ($K_{\mu 2}$) with a 64% branching ratio and $P = 236$ MeV/c, and $K^+ \to \pi^+\pi^0$ ($K_{\pi 2}$) with a 21% branching ratio and $P = 205$ MeV/c. The charged particle spectrum of the major K^+ decay modes is shown in Fig. 1 together with the spectrum from $K^+ \to \pi^+\nu\bar{\nu}$. The $K^+ \to \pi^+\nu\bar{\nu}$ signal can be observed in the region away from these two kinematic peaks. The search described here concentrates on the region between the $K_{\pi 2}$ and $K_{\mu 2}$ peaks.

The only other important background sources are scattering of pions in the beam (either from kaon decay/interaction or pions from the K^+ production target) and K^+ charge exchange (CEX) reactions resulting in decays $K_L^0 \to \pi^+l^-\overline{\nu}$, where $l = e$ or μ.

The detector has been described in detail elsewhere[11]; here, we sketch the main ideas. To achieve the large kinematic suppression of the monochromatic peaks $K_{\pi 2}$ and $K_{\mu 2}$, we work in the kaon rest frame, slowing down a 790 MeV/c kaon beam in a BeO

*See the amusing exchange between B. Winstein and G. Kane in the Sept. 1998 issue of *Physics Today* on a fictitious look back from the year 2011 to the history of particle physics from the late 1990s onward.

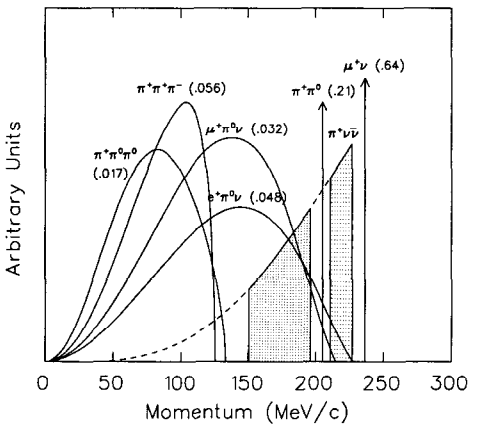

Fig. 1. Charged-particle momentum spectrum in the K^+ rest frame for the major K^+ decay modes and for $K^+ \to \pi^+\nu\bar{\nu}$.

degrader and stopping it in a finely segmented, fully active, scintillating-fiber target. This drives the geometry of the detector, which is cylindrical with endcaps covering the polar regions, much like a colliding-beam detector. Since vetoing of extra energy in the event is a key to the detection strategy, the detector is almost fully active.

The fiducial volume is defined by the Range Stack (RS) scintillators in the barrel region, covering about 50% of the solid angle. The pions from K^+ decay are stopped in the RS scintillator. This allows redundant measurements of track kinematics, namely kinetic energy and range. It also allows for a powerful technique for π/μ separation, which requires the positive identification of the $\pi^+ \to \mu^+ \to e^+$ decay sequence. This is achieved with flash-ADC-based 500-MHz transient digitizers (TD)[12] which digitize the phototube outputs. In addition, dE/dx separation of π from μ can be utilized. Further kinematic rejection is achieved with a momentum measurement in a 1 T solenoidal field, using a low-mass drift chamber[13] with a resolution $\Delta P/P \sim 0.9\%$ at $P = 205$ MeV/c. Efficient rejection of modes with photons is achieved with nearly 4π photon veto coverage, typically about 15 radiation lengths thick, employing a variety of technologies: lead-scintillator sandwich in the barrel region (BV), undoped CsI in the endcaps (EC),[14] lead-glass, lead-scintillator sandwich, and "Shashlik"-type detectors in the beam region. Signals are digitized with 500-MHz CCD transient digitizers[15] based on Ga-As technology. Photon veto time windows are typically a few ns, with energy thresholds ranging from 0.2 to about 3 MeV. For the incoming beam, K/π separation is achieved with a Cherenkov counter with a lucite radiator. Finely segmented tracking and good timing of the beam is achieved with MWPC's (1.27 mm wire spacing), scintillator hodoscopes and a scintillating fiber kaon stopping target (5 mm square fiber), the latter two also digitized by CCD's transient digitizers.

At typical rates, we took about 5 MHz of incoming kaons. These were analyzed by a two-level trigger. The first level provided a rejection factor of about 800 by requiring a kaon stopping in the target, a decay 1.5 ns later, no photons in the BV, EC, or RS, a range longer than $K^+ \to \pi^+\pi^+\pi^-$ and shorter than $K_{\mu 2}$. The second level required a $\pi^+ \to \mu^+$ decay in the counter, where the charged particle stopped and no energy was deposited in the counter radially outward from the stopping counter; this provided a rejection factor of about 20.

The DAQ[16] is Fastbus-based, with front-end readout into SLAC Scanner Processors (SSP). The data is transferred via the cable segment to VME processors and then to a Silicon Graphics (SGI) machine (model number improves with year). The data transfer capability is currently > 25 Mbytes/sec. The deadtime, dominated by the readout of the front-end modules into the SSP's, is currently about 17% per MHz of stopped kaons (down from 28% in 1995).

2.2 Offline Analysis

To elude rejection, $K_{\mu 2}$ and $K_{\pi 2}$ events have to be reconstructed incorrectly in range, energy, and momentum. In addition, any event with a muon has to have its track misidentified as a pion. The most effective weapon here is the TD analysis, requiring observation of the $\pi^+ \to \mu^+ \to e^+$ decay sequence; this provides a muon rejection factor of about 10^5. Events with photons, such as $K_{\pi 2}$ decays, are efficiently eliminated by the photon veto; the rejection factor for events with π^0's is around 10^6. A scattered beam pion can survive the analysis only by misidentification as a K^+ and if the track is mismeasured as delayed, or if the track is missed entirely by the beam counters after a valid K^+ stopped in the target. CEX background events can survive only if the K_L^0 is produced at low enough energy to remain in the target for at least 2 ns, if there is no visible gap between the beam track and the observed π^+ track, and if the additional charged lepton goes unobserved.

The data are analyzed with the goal of reducing the total expected background to significantly less than one event in the final sample. The same data set is used for background studies and for the signal search so that any hardware failures, or time-dependent effects, are naturally accounted for in the background estimates. The offline analysis is performed "blind," in the sense that the signal region is always hidden (by inverting one or more cuts) while cuts are developed and background levels estimated. Without this procedure, it would be difficult to avoid the systematic error, whereby a signal event might be eliminated with minimal acceptance loss by a slight tweaking of one of the more than 50 cuts in the analysis.

To develop the cuts, we take advantage of redundant, independent constraints available on each source of background to establish two independent sets of cuts. One set of cuts is relaxed or inverted to enhance the background (by up to three orders of magnitude) so that the other group of cuts can be evaluated to determine its power for rejection.

For example, $K_{\pi 2}$ is studied by measuring the rejection of the kinematic cuts on a sample of events failing the photon veto, while the photon veto rejection is measured on a sample of events which are kinematically consistent with $K_{\pi 2}$. This is illustrated in Fig. 2. Figure 2(a) shows the range versus energy for events tagged by the presence of photon activity in the detector after removing $K_{\mu 2}$ and beam backgrounds. Figure 2(b) shows the momentum distribution for events kinematically consistent with $K_{\pi 2}$, again after removing $K_{\mu 2}$ and beam backgrounds. The three histograms show the momentum spectra at different levels of photon vetoing: raw spectrum, after the trigger and first pass of the offline analysis, and finally after the final photon veto cuts. To determine the background in the final signal region, the number of events in the signal region in Fig. 2(a) (i.e., two events) is corrected for the tagging efficiency and then divided by the photon veto rejection from Fig. 2(b).

$K_{\mu 2}$ (including $K^+ \to \mu^+ \nu_\mu \gamma$) is studied by separately measuring the rejections of the TD particle identification cuts and the kinematic cuts. The background from beam pion scattering is evaluated by separately measuring the rejections of the beam counter and timing cuts. For the CEX background, events with K^+ charge exchange in the stopping target were collected with a special trigger, triggering on the two pion decay of the K_S^0; these events are then used as input to Monte Carlo studies, replacing the K_S^0 with a Monte Carlo K_L^0.

Small correlations in the separate groups of cuts are investigated for each background source and corrected for, if they exist. An example of the absence of correlation

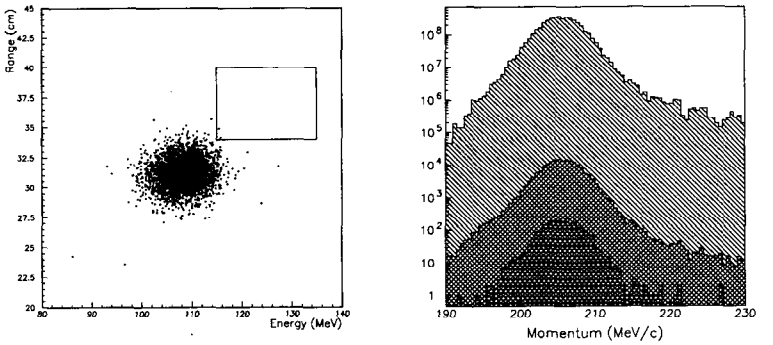

Fig. 2. $K_{\pi 2}$ analysis with the 1995 data. (a) shows the range vs energy for events tagged by the presence of photon activity in the detector after removing $K_{\mu 2}$ and beam backgrounds. (b) shows the momentum distribution for events kinematically consistent with $K_{\pi 2}$ after the removal of $K_{\mu 2}$ and beam backgrounds. The three histograms show the momentum spectra at different levels of photon vetoing: raw spectrum, after the trigger and first pass of the offline analysis, and finally, after the final photon veto cuts.

in the $K_{\pi 2}$ study can be seen in Fig. 2 by noting that in the right plot [Fig. 2(a)], the $K_{\pi 2}$ lineshape does not change as tighter photon veto cuts are applied.

Before looking in the final signal region, likelihood functions for each background type are constructed, using the method described above. For example, the $K_{\pi 2}$ kinematic likelihood function is measured with a sample of events failing the photon veto, while the $K_{\pi 2}$ photon veto likelihood is measured with a sample of events kinematically consistent with $K_{\pi 2}$. These likelihood functions are used to predict the shape of the background distributions outside the final signal region. The prediction is not guaranteed to be satisfied because the final measurement involves the simultaneous application of all likelihood functions; the success of the predictions, therefore, tests the independence of the individual likelihood functions. Finally, the background likelihood functions are used to assess the background likelihood of any candidate events.

3 1995 Results

The results from the 1995 analysis have been published.[4] The key points are summarized here.

The background levels in the 1995 data were estimated with the above procedure to be $b_{K_{\mu 2}} = 0.02 \pm 0.02$, $b_{K_{\pi 2}} = 0.03 \pm 0.02$, $b_{beam} = 0.02 \pm 0.01$, and $b_{CEX} = 0.01 \pm 0.01$ for a total background of $b = 0.08 \pm 0.03$ events.

As a cross-check of the background estimates and of the shapes of the background distributions near the signal region, the background likelihood functions were used to estimate the number of events expected to appear when the cuts were relaxed in predetermined ways, so as to allow orders of magnitude higher levels of all background types. At approximately the $20 \times b$ level, we observed two events where 1.6 ± 0.6 were expected. At the level $150 \times b$, we found 15 events where 12 ± 5 were expected. The events which were admitted by the relaxed cuts were consistent with being due to the known background sources.

Figure 3(a) shows the range versus energy for the events surviving all other analysis cuts. Only events with measured momentum in the accepted region $211 < P < 230$ MeV/c are plotted. The rectangular box indicates the signal region specified as range $34 < R < 40$ cm of scintillator and energy $115 < E < 135$ MeV. One event was observed in the signal region. The residual events below the signal region clustered at $E = 108$ MeV were due to $K_{\pi 2}$ decays where both photons had been missed. The number of these events was consistent with estimates of the photon detection inefficiency.

The event satisfied the tightest background likelihood criteria designed in advance for candidate evaluation. This put the event in a region where $b' = 0.008 \pm 0.005$ events would be expected from known background sources while 55% of the final acceptance for $K^+ \to \pi^+ \nu\bar{\nu}$ would be retained.

The acceptance for $K^+ \to \pi^+ \nu\bar{\nu}$ was $A = 0.0016 \pm 0.0001(stat.) \pm 0.0002(sys.)$, determined mainly from calibration data taken simultaneously with the physics data. Monte Carlo was used to obtain the acceptance factors only for solid angle, $K^+ \to \pi^+ \nu\bar{\nu}$ phase space, and losses from π^+ nuclear interactions and decays in flight. Figure 3(b) shows the simulated R versus E distribution for $K^+ \to \pi^+ \nu\bar{\nu}$ with the final analysis cuts applied. The acceptance was cross-checked by a parallel measurement of the $K_{\pi 2}$ branching ratio, comparing it to the world-average value. The total exposure of the 1995 run was $N_{K^+} = 1.49 \times 10^{12}$ kaons entering the stopping target. The resulting branching ratio is $B(K^+ \to \pi^+ \nu\bar{\nu}) = 4.2^{+9.7}_{-3.5} \times 10^{-10}$, assuming that the one event observed is from $K^+ \to \pi^+ \nu\bar{\nu}$.

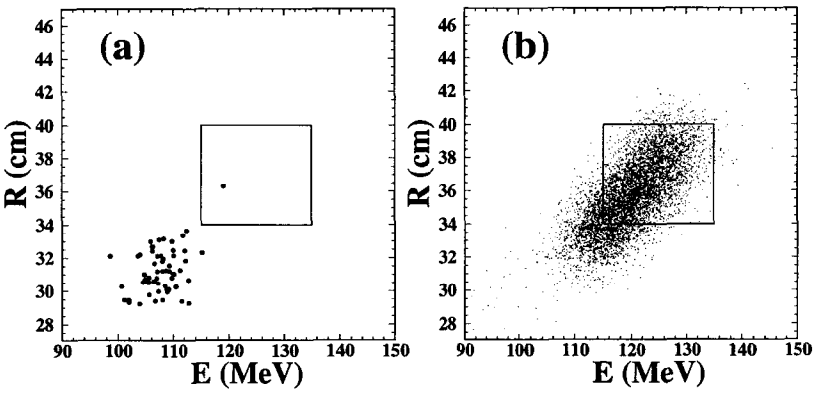

Fig. 3. (a) Range R vs energy E distribution for the $K^+ \to \pi^+ \nu\bar{\nu}$ data set (1995) with the final cuts applied. The box enclosing the signal region contains a single candidate event. (b) The Monte Carlo simulation of $K^+ \to \pi^+ \nu\bar{\nu}$ with the same cuts applied.

The candidate event was kinematically inconsistent with a massless X^0. The χ^2 C.L. for consistency with the hypothesis of a massless X^0 was 0.8%. The acceptance was $A_{K^+ \to \pi^+ X^0} = 0.0052 \pm 0.0003(stat.) \pm 0.0007(sys.)$. Based on no events observed in the region $221 < P < 230$ MeV/c, we set a 90% C.L. upper limit $B(K^+ \to \pi^+ X^0) < 3.0 \times 10^{-10}$ for a massless X^0.

4 Post-1995 Developments

4.1 Online Improvements

To increase the sensitivity per hour, the basic strategy in the post-1995 running of E787 has been to run with a lower K^+ momentum and remove BeO degrader material. This decreases the probability that the incoming kaon is lost in the BeO degrader (from multiple Coulomb scattering and interactions), reducing the accidental rate in the detector and increasing the fraction of kaons reaching the stopping target. Simultaneously, the proton flux on the kaon production target was increased to maintain the overall kaon flux. In addition, improvements were made to the trigger, reducing the deadtime frac-

tion from 28% to 17% per MHz of stopped kaons. The efficiency of the second-level trigger ($\pi^+ \to \mu^+$) was increased by a factor of 1.27 over 1995. A further gain of a factor of 1.05 was achieved by extending the time range recorded by the TD's to look for the electron from $\mu^+ \to e^+$ decay.

In the ongoing 1998 run, the AGS duty factor was improved by a factor of 1.1 by going from a 1.6 sec spill every 3.6 sec to a 2.2 sec spill every 4.5 sec. The number of protons per spill was increased to maintain the kaon flux. In addition, a better operating point was found by careful optimization in the space of K momentum, spill length and protons on target. The result of these factors is summarized in Fig. 4, which shows the increase in sensitivity/hour from year to year. The sensitivity/hour for the ongoing run is about a factor of two better than the 1995 running conditions. The sensitivity/hour is limited by proton intensity, currently about 30×10^{12} protons per spill (30 Tp) onto our kaon production target. Intensities which would increase the sensitivity/hour by a factor of three times better than the 1995 value have been demonstrated to be within the current capabilities of the AGS.

The total exposure in the 1996 and 1997 runs amounted to about 1.5 times the 1995 exposure. The increase in sensitivity/hour was offset by a decrease in running time: 17 weeks in 1996 followed by nine weeks in 1997, compared to 22 weeks in 1995. The current run, however, is expected to last 27 weeks and to result in an exposure five times that of the 1995 run. This would imply a total exposure in 1995-1998 which is 7.5 times that of the 1995 run alone, or a single-event sensitivity of 0.7×10^{-10}.

4.2 Offline Analysis

The goal of the offline analysis is to increase the rejection to maintain the signal-to-noise ratio as the overall sensitivity grows, while maintaining (or possibly even increasing) the acceptance at the same time.

Better range resolution in both the Gaussian core and in the tails was achieved with tracking improvements in the range stack and target. The range tail for $K_{\pi 2}$ events is shown in Fig. 5; a significant reduction in the background level is apparent.

For the $K_{\mu 2}$ background, a more sophisticated dE/dx analysis was developed for the range stack, reducing the number of $K_{\mu 2}$ events downshifting in range and energy due to nuclear interactions. Tracking improvements in the drift chamber and better tracking quality cuts reduced the momentum tail. On the TD side, better understanding of the different sources of TD background in the $K_{\mu 2}$ peak compared to $K^+ \to \mu^+ \nu_\mu \gamma$ and

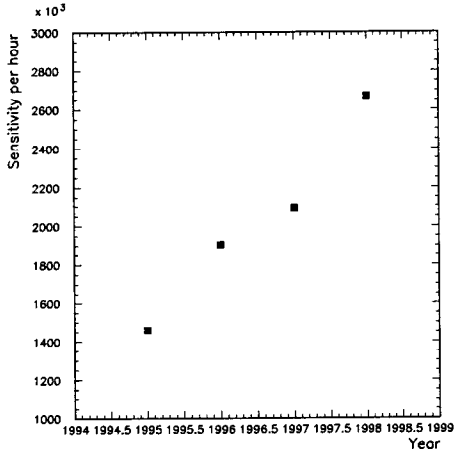

Fig. 4. Sensitivity per hour as a function of year.

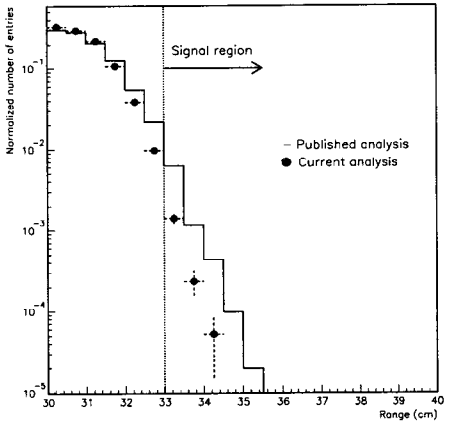

Fig. 5. $K_{\pi 2}$ range tail in the current analysis, compared to the published analysis.

$K^+ \to \mu^+\pi^0\nu_\mu$, and a better algorithm for finding the electron from $\mu^+ \to e^+$ decay resulted in a 17% gain in acceptance for the same level of rejection as the published analysis. The beam background was lowered by improved cuts against kaons decaying in flight in the stopping target, improved use of the CCD information in the target, and better cuts against two kaons entering the detector closely spaced in time. The CEX background was lowered by the above-mentioned improvements in the target tracking and by a likelihood analysis utilizing information in the target and beam hodoscopes.

In total, a preliminary assessment indicates that the overall background levels can be reduced by a factor of three with no loss in acceptance. This would imply a background level, stated as a branching ratio, of 1.1×10^{-11}.

5 Conclusion

The E787 Collaboration has published evidence for the decay $K^+ \to \pi^+\nu\bar{\nu}$ based on one clean event seen in the 1995 data sample. Analysis is proceeding on the 1996-1997 data set, which has an exposure 1.5 times larger than the 1995 data set alone.

In the ongoing 1998 run, extrapolating the current running conditions, the exposure is expected to reach five times that of 1995, for a total sensitivity (1995-1998) reaching 0.7×10^{-10}. Preliminary indications are that background levels can be held down to the level of 1.1×10^{-11} with no loss in acceptance compared to the 1995 run.

A new experiment, based largely on E787 with only modest upgrades and further improvement in the duty factor (and proton intensity), aims to reach a sensitivity of $(0.07 - 0.13) \times 10^{-12}$ with two years of AGS running in the RHIC era.[17] This proposal (E949) was recently approved by the BNL PAC.

References

[1] M. Kobayashi and T. Maskawa, Prog. Theor. Phys. **49**, 652 (1973).

[2] A. J. Buras and R. Fleischer, in *Heavy Flavors II*, edited by A. J. Buras and M. Lindner (World Scientific, 1997). Also hep-ph/9704376.

[3] G. Buchalla *et al.*, Rev. Mod. Phys. **68**, 1125 (1996).

[4] S. Adler *et al.*, Phys. Rev. Lett. **79**, 2204 (1997).

[5] Among many examples, Y. Nir and M. Worah, Phys. Lett. B **423**, 319 (1998); A. J. Buras, A. Romanino, and L. Silvestrini, Nucl. Phys. B **520**, 3 (1998); G. Colangelo and G. Isidori, J. High Energy Phys. **9809**, 9 (1998).

[6] K. Agashe and M. Graesser, Phys. Rev. D **54**, 4445 (1996).

[7] G. Buchalla *et al.*, Phys. Rev. D **53**, 5185 (1996).

[8] F. Wilczek, Phys. Rev. Lett. **49**, 1529 (1982).

[9] J. Preskill, M. B. Wise and F. Wilczek, Phys. Lett. B **120**, 127 (1983); L. F. Abbott and P. Sikivie, *ibid*, 133 (1983); M. Dine and W. Fischler, *ibid*, 137 (1983).

[10] M. Hindmarsh and P. Moulatsiotis, hep-ph/9807363.

[11] M. S. Atiya *et al.*, Nucl. Instrum. Methods A **321**, 129 (1992) describes the original E787 detector. References 12-16 describe most of the upgrades for the current detector.

[12] M. S. Atiya *et al.*, Nucl. Instrum. Methods A **279**, 180 (1989).

[13] E. W. Blackmore *et al.*, Nucl. Instrum. Methods A **404**, 295 (1998).

[14] I.-H. Chiang *et al.*, IEEE Trans. Nucl. Sci. **NS-42**, 394 (1995); T. K. Komatsubara *et al.*, Nucl. Instrum. Methods A **404**, 315 (1998); M. Kobayashi *et al.*, Nucl. Instrum. Methods A **337**, 355 (1994).

[15] D. A. Bryman *et al.*, Nucl. Instrum. Methods A **396**, 394 (1997).

[16] M. Burke *et al.*, IEEE Trans. Nucl. Sci. **NS-41**, 131 (1994); C. Witzig and S. Adler, Real-Time Comput. Appl. **123** (1993); S. Adler, Int. Conf. Electr. Part. Phys. **133** (1997); C. Zein *et al.*, Real-Time Comput. Appl. **103** (1993).

[17] See "http://www.phy.bnl.gov/e949/e949.html".